



Full-length article

Increased shielding of a Direct Energy Deposition process to enable Deposition of reactive materials; an investigation into Deposition of 15-5 PH Stainless Steel, Inconel 718 and Ti-6Al-4V

Nikolaos Tapoglou*, Joseph Clulow, David Curtis

Advanced Manufacturing Research Centre (AMRC), University of Sheffield, Advanced Manufacturing Park, Wallis Way, Catcliffe, Rotherham S60 5TZ, United Kingdom

ARTICLE INFO

Article history:
Available online 9 December 2020

Keywords:

Direct energy deposition
Hybrid manufacturing
Titanium alloy
Ti6Al4V
Stainless steel
Inconel 718

ABSTRACT

Hybrid additive and subtractive machining combines the flexibility of additive manufacturing (AM) with the high precision and geometrical accuracy of computer numerical control (CNC) machining. Of the many metal AM strategies blown powder direct energy deposition (DED) is the method most commonly chosen for incorporation into hybrid additive and subtractive platforms. Due to the necessity for coolant during machining operations, these platforms are usually not sealed environments meaning the deposition of reactive metals such as titanium to acceptable standards is not possible due to oxygen absorption from the surrounding environment. The research presented focuses on the investigation of the effect of a series of shielding methods in the geometry and microstructure of the materials deposited in a hybrid-manufacturing platform. The ultimate objective is to select the method with the biggest potential to enable the deposition of reactive materials with the aim of successfully depositing low oxygen content titanium, enabling the creation of Ti-6Al-4V at grade 5 and grade 23. To achieve this, bath and bag shielding strategies were compared with the standard through nozzle shielding when depositing in 15-5 PH stainless steel, Inconel 718 and Ti-6Al-4V. Based on the results of the post machining analysis the oxygen content of a multi-layer titanium sample was found to be 0.079%, lower than the maximum limit for grade 23 Ti-6Al-4V.

© 2020 CIRP.

Introduction

Traditional manufacture relies on forging, casting and rolling of bulk feedstock materials along with subtractive machining to final geometries. This can result in large volumes of wasted material, long machining processes, multiple set-ups and high tooling costs. Additive manufacturing (AM) technologies have the capability to significantly reduce buy-to-fly ratios giving manufacturers the ability to create near-net shape parts, reducing the volume of rough machining required in many applications [1]. Additionally, hybrid additive and subtractive machining centres (HMCs) offer the ability to drastically reduce supply chain size and lead time by manufacturing the part in a single set-up.

Due to its versatility, powder-based direct energy deposition (DED) is the AM technology most commonly chosen for use in HMCs [2]. However, due to the need for coolant during machining operations, DED technology uses only local shielding. As opposed

to completing deposition inside a sealed, purged environment, as some blown powder DED platforms [3,4]. For reactive materials, such as titanium, local shielding alone is not enough to prevent oxygen absorption during solidification and cooling of newly deposited and re-melted weld material.

The capability to deposit titanium alloys on HMCs would be of use to a number of high-value manufacturing industries, where it has become a widely used and dependable material due to the low density, low Young's modulus, good mechanical properties and good corrosion resistance [5–7]. The most common of which is Ti-6Al-4V, developed for the aerospace industry the alloy is now a mainstay in other industries such as automotive, marine, energy, biomedical and chemical [8,9].

For titanium, exposure to oxygen during deposition compromises the chemical composition of the weld, making it appear grey and porous [10]. The high affinity of titanium with oxygen and nitrogen means that the build environment also has a large role to play in governing the strength of AM titanium.

A mole fraction of as much as 0.30 oxygen can be dissolved in α -Titanium before an oxide is formed. When oxygen content increases both the α -transus and the β -transus temperatures

* Corresponding author.
E-mail address: n.tapoglou@sheffield.ac.uk (N. Tapoglou).

increase. Due to the large oxygen solubility of titanium, all titanium alloys will contain a non-negligible amount of oxygen absorbed during processing. The metal powders used in AM are no exception to this, with the further processing of metal powders through AM a further opportunity for oxygen contamination [11].

In Ti-6Al-4V, oxygen atoms are located in the interstitial sites of the lattice, which results in higher strength due to the strengthening and stabilisation of the α -phase. Too high a concentration of oxygen however results in diminishing ductility [6,12]. Controlling the oxygen during deposition is good for improving the elongation properties of the material [13], the failure of which is strongly dependent on microstructure.

For the DED process, the thermal history of the deposited material has a significant impact on the microstructure, such as morphology and grain size. This is due to the high heating/cooling rates, significant temperature gradients, and bulk temperature increment. The solidification rate of the melt pool, the thermal gradient at the interface solid-liquid and the ratio between the cooling rate and the gradient of temperature define the microstructure of a deposited part after solidification [2]. As with most layer metal deposition (LMD) of metals, Ti-6Al-4V components usually consists of large elongated grains growing towards the heat source (i.e., the build or z-direction). In the case of Ti-6Al-4V, these are prior β grains. This results in differing material properties, particularly for tensile and fatigue testing. Measuring properties in a specimen fabricated in the build direction, parallel to the elongated prior β -grains, results in a lower volume fraction of grain boundaries in comparison with a specimen fabricated in the scanning direction (x/y plane). It has been theorised, that these boundaries act as potential failure initiation points, and are the reason behind reductions seen in elongation for samples in the scanning direction as compared to the build direction due to prior β -grain boundaries being normal rather than parallel to the load [12]. This was also seen by Keist et al. when tensile testing samples taken from wall structures [14].

The majority of AM Ti-6Al-4V created using powder feedstock is achieved through powder bed fusion (PBF), which can achieve intricate internal features, with low levels of porosity and defects. PBF however, is not suitable for large components or for adding to large or irregular components. For this reason, the deposition of Ti-6Al-4V using wire or blown powder DED creates opportunity for the creation and repair of many larger structures, currently restricted to large subtractive machining processes or long lead time, complicated casting operations [2,7,15].

The oxygen present in finished LMD Ti-6Al-4V components typically originates from the oxygen dissolved in the initial powder

and the oxygen entrapped in the part during its various steps of handling and processing [12]. The findings of Jun Yu et al. [6] seem to suggest that through increasing the shielding gas flow rate and the use of low laser powers, sufficient shielding is given to the melt pool during solidification and cooling to prevent oxygen absorption. It is worth noting that the effect of shielding gas flow rate on the process parameters for weld quality is crucial in blown powder DED [16].

The high density of argon compared to air helps it to push away oxygen [10] and remain over the weld zone after the laser head has moved away. However, this is not usually sufficient enough to prevent oxygen absorption when depositing reactive materials such as titanium. An increase in shielding gas flow rate could also assist with the cooling of the melt pool as in the DED process, heat dissipates from the melt pool via conduction downwards as well as forced convection by the shielding gas flows [8]. It is common that a well shielded laser clad bead would show a light silver-straw colour, as opposed to the dark dull colour caused by oxidation [17], as is stated in the titanium fusion welding standards for an indication of good quality welds [8].

Amado et al. [18] state that on laser deposited titanium alloys this contamination is rather limited due to the fast cooling rates involved in the process. Absorbed oxygen was only being detected within a few microns beneath surface and was removed by common post processing procedures such as cleaning, polishing or machining the deposited layers. While this is true in the case of single layers, laser deposition of titanium with overlaying several layers and multi-layer deposition poses a risk of oxygen absorption through the reheating of the weld material. In processes where single tracks exhibit clear signs of oxidation in the form of, for example, a violet oxide scale the oxidation problem is amplified, as seen on the surface of samples deposited by Amado et al. [18]. This scale can generally be removed and cleaned by wire brushing, which is also acceptable according to the welding standards [17]. Amado et al. suggested that for multi-layer samples an enclosed inert gas chamber or, at least, cleaning procedures between depositions of successive layers would be needed [18].

Eo et al. completed DED deposition trials with 316L stainless steel varying the argon shield gas flow rate between 5 and 25 L/min, for two deposition parameter settings. It was found that oxygen content decreased with an increase in the shielding gas flow rate in both conditions, as would be expected. Oxygen content of the AM was larger than forged steel for all deposition conditions, with the least oxygen content found to 375 ppm [19].

The study found the melt pool shape varied due to the different oxygen content in the melt pool, caused by the varied shielding gas

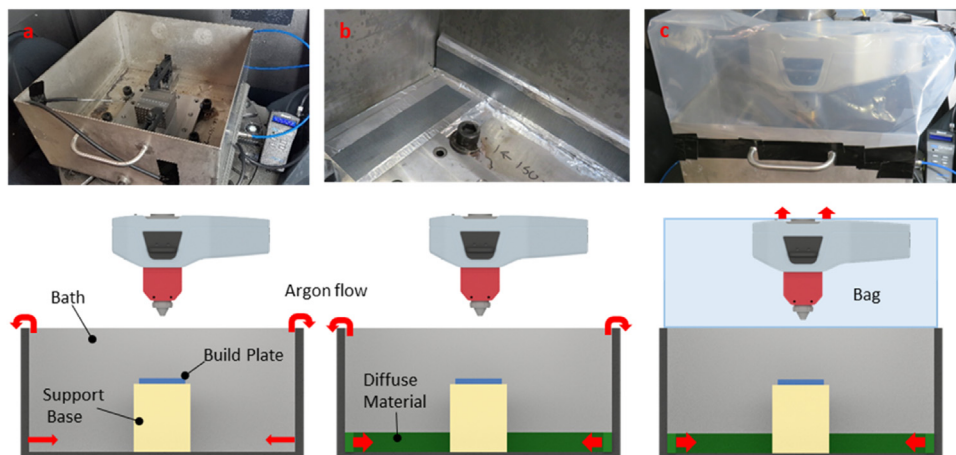


Fig. 1. Experimental setup (a) Bath (b) Diffused bath (c) Bag.

flow rate. This resulted in the melt pool temperature being significantly affected by the oxidation kinetics. It could also be seen that the increased levels of shielding gas flow rate, 15–25 L/min caused much greater levels of weld penetration into the substrate [19].

In this research, three shielding methods were tested for their ability to provide shielding during the deposition process. The main focus was to prevent the absorption of oxygen into the deposited material, therefore enabling the creation of improved quality alloys in terms of material composition, internal defects and surface finish compared to the standard blown powder deposition process using limited shielding. While bath [20] and bag [21] shielding mechanisms have been trialled for AM processes in previous literature, the novelty of the proposed approach lies in the fact that the shielding of both has been compared and retrofitted onto a commercially available hybrid machining platform, enabling the deposition and machining of reactive materials on the same platform.

Experimental method

The DMG Mori Lasertec 65 3D Hybrid integrates additive manufacturing deposited by blown powder into a 5-axis milling machine, combining the flexibility of the laser metal deposition process with high precision cutting capabilities. The system provides local shielding delivered through the deposition nozzle in the form of argon gas. In order to increase shielding, three shielding conditions were trialled;

- A bath (Fig. 1a); argon is delivered into the bath in two locations via push fit fittings on opposite sides of the bath. The argon is then distributed into the bath from these inlets through 60 holes located along on the bottom and sides of the bath. The weight of the argon results in the argon sitting in the bath, pushing the oxygen out the top.
- A diffused bath (Fig. 1b); In order to enable a greater gas flow rate without creating turbulence which could detrimentally effect

the oxygen level in the bath or the powder flow a diffusing medium was added over the argon outlets in the bath. This was created using a three layer sandwich construction with a wire wool layer between two perforated steel sheets containing 1 mm diameter holes.

- A bag (Fig. 1c); using 800 gauge polythene sheeting a semi-sealed bag solution was created. By supplying argon at an over pressure the oxygen inside the bag is pushed out, creating an argon environment.

The PRO OX-100B oxygen monitoring kit was used to take readings inside the deposition environment down to 100 PPM (0.01%), equipped with a Bluetooth transmitting device that allows the monitor to send the oxygen readings wirelessly to the data capturing platform. The oxygen sensor was positioned 20 mm from the base plate at base plate level in order to try get the most accurate readings for oxygen levels at the deposition region.

The powders used for deposition during the experiments were:

- 15-5PH stainless steel (Oerlikon MetcoAdd 15-5 PH)
- Inconel 718 (Oerlikon MetcoAdd 718F)
- Ti-6Al-4V (Carpenter Additive CT POWDERRANGETI64 E)

Table 1 shows the chemical composition of each powder used in the deposition trials, all powders had the same sieve range to provide powder particles between 45 and 106 μm in diameter.

The trials were split into three phases. The first phase concentrated on testing the performance of the shielding solution. Phase 2 tested the shielding solutions through deposition of the non-reactive materials 15-5PH stainless steel (Phase 2.1) and Inconel 718 (Phase 2.2), comparing the performance of each shielding condition previously described with the standard local shielding. Phase 3 applied the results of Phase 1 and 2 in order to deposit Ti-6Al-4V powder, depositing solely in the bag solution. The argon flow rate for all bath depositions was 30 L/min, while for diffused bath and bag depositions the flow rate used was 45 L/min.

Table 1
Chemical composition and sieve range for each material.

Element	Material (in weight %)			Measurement Method
	15-5 PH	Inconel 718	Ti-6Al-4V	
Ag		<0.0001		ICP-MS
Al		0.44	6.00	ICP
B		<0.006		ICP
Bi		<0.0001		ICP-MS
C	0.03	0.05	0.08	Combustion
Ca		<0.01		ICP-MS
Co		0.04		ICP
Cr	14.66	18.90		ICP
Cu	3.30	<0.10		ICP
Fe	76.00	18.10	0.25	Balance/ICP
H			0.0120	ICP
Mn	0.49	0.08		ICP
Mo	<0.1	3.05		ICP
Mg		<0.01		ICP
N	<0.1	0.02	<0.03	LECO
Nb	0.28	5.10		ICP
Ni	4.52	53.40		ICP
O	0.022	0.01	<0.13	LECO
P	0.013	<0.010		ICP
Pb		<0.0001		ICP-MS
S	<0.010	<0.010		Combustion
Se		<0.001		ICP-MS
Si	0.50	<0.01		ICP
Ta		<0.01		ICP
Ti		0.88	Balance	ICP
V			4.00	ICP
Y			0.005	ICP
Sieve range	45 – 106 (μm)	45 – 106 (μm)	45 – 106 (μm)	

Each phase consisted of the deposition of single tracks, multi-track layers and multi-layer depositions, with the results from each enabling a down selection for the following. The parameters used for the single track deposition can be seen in Table 2.

The deposited samples were visually inspected and then sectioned, polished and etched to reveal the dilution, heat affected zone, pores and cracks present in the builds. The sectioned areas were examined with a Leica DSM1000 microscope.

Results & discussion

Phase 1: shielding performance

The effectiveness of the bath (Fig. 1a), diffused bath (Fig. 1b) and bag (Fig. 1c) shielding solutions were tested, measuring the lowest achieved oxygen levels both before and during deposition. Fig. 2 shows the diffusing material added to the floor and walls of the bath construction, this enabled an increase in the argon flow rate from 30 L/min to 45 L/min without detrimental effects to the laser deposition system that would be caused by turbulent argon gas flow. This increase in the flow rate can be seen in the time taken for each solution to lower the oxygen level from the atmospheric value of 20.9% to the lowest achievable value as shown in Fig. 2. It can be seen that the diffused bath reached a lower minimum oxygen level quicker than the standard bath due to the increased flow rate, however, in all cases, the environment was purged relatively quickly.

The time to return to a safe level for the operator of 19.5% was also monitored. The value of 19.5% was taken from the Respiratory Protection Standard, Occupational safety and Health Administration (OSHA), where an atmosphere with an oxygen content below 19.5% by volume is considered oxygen deficient [22]. Fig. 3 shows that the addition of the diffusing material results in a slower return to atmospheric oxygen levels, while the bag further inhibits the rise in oxygen level. However, due to the relatively higher density of argon, the oxygen level remained low inside the confines of the bath. In areas slightly outside or above the bath, the oxygen level recorded to be above 19.5% and often was the 20.9% atmospheric norm.

Fig. 4 shows oxygen readings taken during the deposition of multi-track layers in the bath, diffused bath and bag shielding setups. The blue dashed lines indicate the start and finish of the deposition. Prior to deposition, it can be seen that the bag has enabled the lowest oxygen level (100 PPM), while the diffused bath has reduced the oxygen level to 4000 PPM and the standard bath to 12,000 PPM.

This figure shows the higher flow rate (45 L/min instead of 30 L/min) permitted by the diffusing material placed over the argon outlet holes enabled a drop in oxygen levels by around 7000 PPM when comparing the diffused bath with the standard bath. It can however be seen that at the start of deposition the oxygen level increases, continuing to do so during the deposition at the same rate for both the standard and diffused bath shielding set-ups. With the standard bath reaching a peak oxygen level of 4.5%, while the diffused bath peaking at 3.4%. In comparison the bag shielding set-up shows relatively very little fluctuation compared to the bath

setups, maintaining oxygen levels below 300 PPM. This increase in oxygen level during deposition for the bath and diffused bath setups was attributed to the movement of the laser head which is disrupting the argon pool inside the bath and pulling in oxygen from outside the bath.

Phase 2: non-reactive materials

Phase 2 trials compared the effectiveness of the shielding solutions at reducing oxygen absorption during and after deposition. The deposition of single track welds in 15-5 PH stainless steel and Inconel 718 was performed using the parameters shown in Table 2 for each shielding condition. There was no noticeable difference in weld geometry depending on the level of shielding. There was however a notable change in the colour of the surface of the weld and in the number of partially melted, adhered powder particles on the weld surface. The number of which appeared to be lower on the samples deposited in increased shielding, leading to an improved surface.

Four sets of parameters were down selected for both materials for the deposition multi-track layer samples. The presence and effect of oxygen can be seen through discoloration of the weld surface. For commonly welded materials this discoloration can form part of the pass/fail criteria [17]. The discoloration differs depending on the material and amount of oxygen present during deposition and solidification. This is evidenced in Table 3 which presents the level of discoloration present in the stainless steel and Inconel multi-track layer samples at varying oxygen levels.

Table 3 shows that in general as the oxygen level in the deposition environment reduces the colour of the surface of the weld changes from a dull grey at atmospheric oxygen levels, through straw coloured when depositing around the 2% oxygen region, to a blue and occasionally purple colour at depositions between 0.1% and 1%. Finally, for very low levels of oxygen (100 PPM), almost no discoloration can be seen. The recorded oxygen levels during deposition (Fig. 4) and the images shown in Table 3 show that the bag shielding solution was the best performing shielding solution.

Cross sections of the multi-track layers and multi-layer stainless steel and Inconel were taken from samples deposited in the bag shielding set-up and with no additional shielding. It was observed in the stainless steel layer deposition that the use of the bag shielding strategy had resulted in a much more stable amount of penetration across the sample, whereas the samples deposited using standard shielding were seen to oscillate between 0.9 mm and 1.4 mm weld layer height. One proposed theory for this is that more laser power is required for the cladding of stainless steel in an argon environment, however not enough deposition was completed in this trial to confirm this theory. There was no pattern seen between the use of increased shielding and either an increase or decrease in sample defects. In general, defects were uncommon in the samples with some large pores visible in a few specimens; however, no cracking was present.

Fig. 5 and Fig. 6 show the grain structure of the multi-layer samples for stainless steel and Inconel 718, respectively, deposited in the bag shielding setup. The Inconel 718 sample in Fig. 6 shows

Table 2
Single track deposition parameters for each phase of trials.

Parameter	Phase 2.1	Phase 2.2	Phase 3
Laser power (W)	2000, 2200, 2400	1800, 2000, 2200	1400, 1600, 1800, 2000
Powder flow (g/min)	11, 12.5, 14	13, 15, 17	4, 6, 8, 10, 12
Shield gas flow (l/min)	5	5	5
Argon flow (l/min)	0, 30, 45	0, 30, 45	45
Feed rate (mm/min)	1000	1000	1000

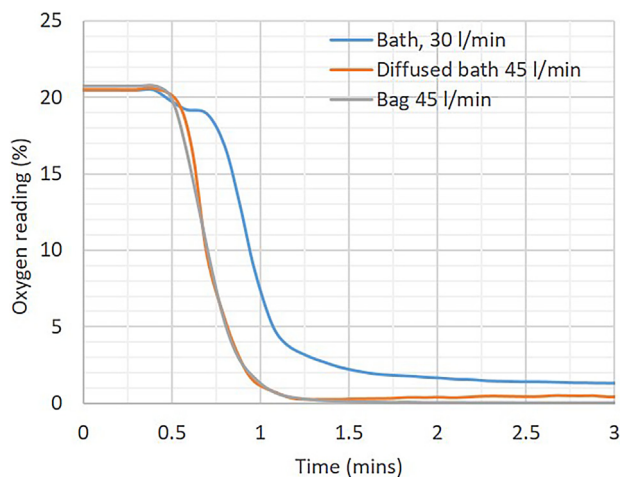


Fig. 2. Oxygen level during purging of deposition area.

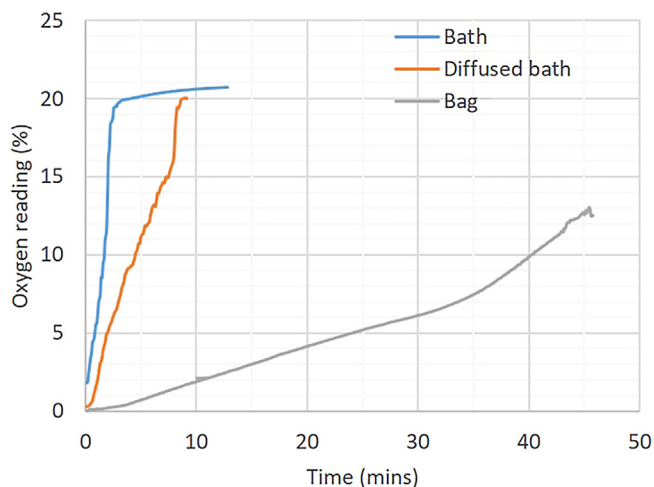


Fig. 3. Oxygen level after argon flow is stopped.

evidence of very long columnar grains growing in the build direction, across multiple layers, as is common in DED material [12]. The effect of the wrap around that is used to maintain the geometrical accuracy of the walls in multi-layer structures could be seen on macro images of the sections.

Post-deposition analysis was performed on the deposited samples in order to understand the oxygen absorption on the samples deposited in the local shielding and bag shielding setups. The oxygen and nitrogen levels were measured using instrumental gas analysis (IGA). Table 4 presents the results for the analysis performed on the stainless steel 15-5PH samples and the Inconel 718 samples. As it can be observed, the nitrogen pickup remains stable between the two shielding methods that were examined. The oxygen pick up is much lower for both the Inconel and Stainless steel samples deposited in the bag shielding setup compared to the local shielding setup.

Phase 3: titanium alloy

The phase 3 trials were completed using the bag shielding only investigating a wider range of deposition parameters. An example

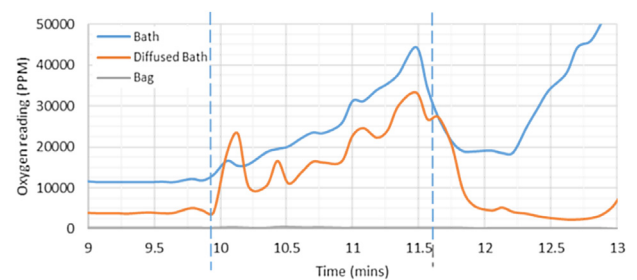


Fig. 4. Oxygen level during deposition of multi-track layers.

of some of the deposited Ti-6Al-4V tracks can be seen in Fig. 7, where no signs of oxidation are present. Fig. 8 shows a section view of a single track, where no cracking or porosity was present. The grains can be seen to be growing in the direction of the heat source as expected.

The effect of the deposition parameters on the weld track geometry, in the form of weld track width, height, penetration and heat affected zone (HAZ) is shown in the surface plots in Figs. 9 to 12.

Fig. 9 shows that the track width increases with laser power and powder flow rate, with the laser power appearing to have a slightly greater impact on track width than the powder flowrate. While for Fig. 10 it can be seen that the track height increases with the powder flow rate, with laser power having comparably a very small effect. Figs. 11 and 12 show the relationship between the weld penetration and HAZ. It can be seen that they both increase with the laser power, as more heat is placed into the part.









Fig. 13 shows an image of the surface of the deposited titanium layer samples, again showing no discoloration. The section view, as seen in Fig. 14, showed no sign of cracking, porosity or other defects. The grain structure can be seen to contain grains growing in the z direction, across the deposited weld beads, with the overlap of weld beads causing the slight waviness of both fusion line and HAZ. It can be noticed that the sample increases in thickness towards the left hand side, the last deposited overlapping track. This is common and is the reason that when depositing multi-layer specimens the build orientation is rotated in order to maintain an even upper surface [23]. This can be caused if the x/y step over is slightly too small, but also happens due to the accumulation of heat into the part during deposition improving the powder catchment.

Table 5 shows the measured layer height for each deposited layer sample. Measurements were taken using the on machine inspection probe, measuring in three evenly spaced locations across the length of the surface of each layer sample. The data shows that the layer samples also increase in height towards one end. As with the increase in height across the width, this increase along the length of the layer sample is also usually caused due to the build-up of heat allowing for greater powder catchment and an increase in layer weld thickness. The layer samples were deposited using a zig-zag strategy, meaning that the start and end position of each track was alternated in order to manage this. However, the data in Table 5 shows that there is still a noticeable increase in height towards one end of the deposition.

Using further down selected parameters multiple layers were deposited on top of each other, rotating the orientation of the deposition 90° every layer in order to manage heat input and ensure geometrical accuracy and symmetry, to create cuboids of 30 × 30 × 25 mm in size. Fig. 15 shows an image of the deposited multi-layer Ti-6Al-4V sample.

Fig. 16 shows the microstructure of a multi-layer titanium sample. Fig. 16b shows the microstructure of a multi-layer

Table 3
Images of weld discoloration at varying oxygen levels.

PPM Oxygen %	100 0.01%	10,000 1%	20,000 2%	209,000 20.9%
15-5 PH Stainless steel				
Inconel 718				

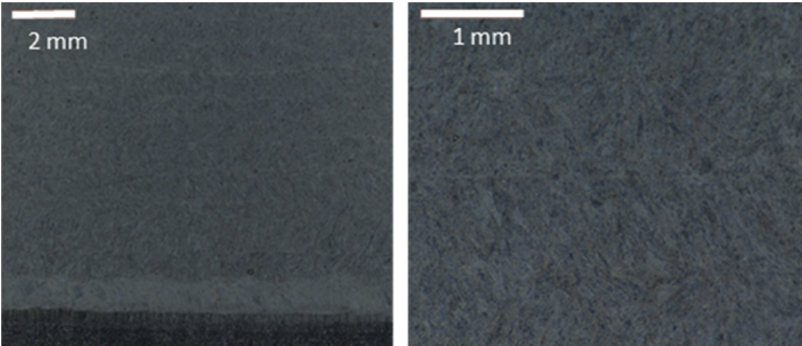


Fig. 5. Microstructure of Stainless steel multi-layer sample.

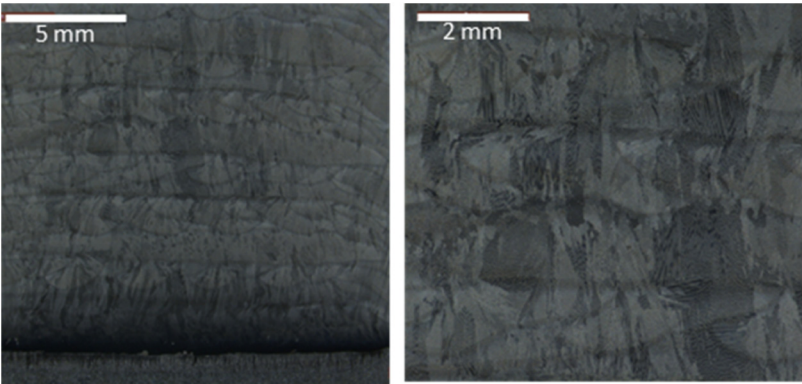


Fig. 6. Microstructure of Inconel 718 multi-layer sample.

titanium sample in the centre of the deposited material around 10 mm from the baseplate.

Titanium microstructure contains a mix of α -phase with a hexagonal closed packed (HCP) crystal structure and β -phase with a body centred cubic (BCC) structure. When rapidly cooled down from high temperatures, as is the case in blown powder DED, the

β -phase can transform into a martensitic α phase with a HCP crystal structure and a $P6_3/mmc$ space group [12].

The samples again showed large columnar grains that grow epitaxially along the deposition direction and span multiple layers, as was the case with the stainless steel and Inconel samples and as found in literature [14], which for titanium are prior- β columnar

Table 4
Nitrogen and oxygen levels on deposited non-reactive alloys using two shielding methods.

Shielding	Local shielding		Bag shielding	
	Nitrogen	Oxygen	Nitrogen	Oxygen
15-5 PH	0.017%	0.058%	0.017%	0.024%
Inconel 718	0.019%	0.026%	0.021%	0.009%

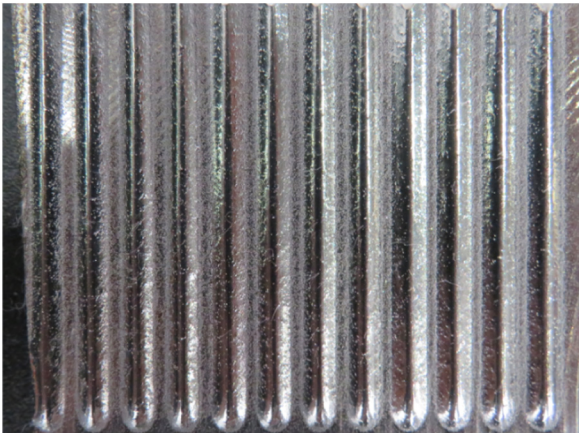


Fig. 7. Ti-6Al-4V Single track deposition (1600 W to 2000 W, 6 to 10 g/min).

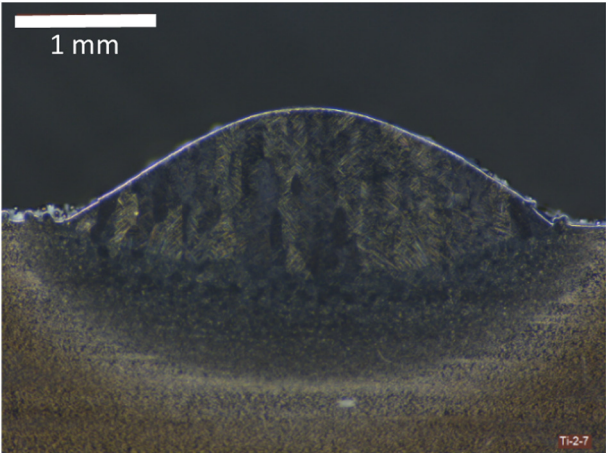


Fig. 8. Sectioned, etched view of Ti-6Al-4V Single track.

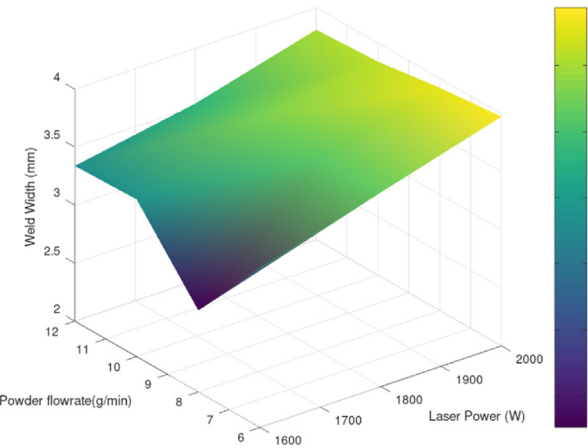


Fig. 9. Ti-6Al-4V single track width (mm) against laser power (W) and powder flow rate (g/min).

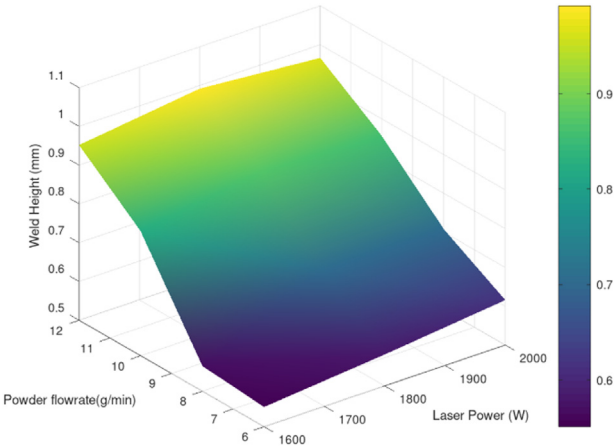


Fig. 10. Ti-6Al-4V single track height (mm) against laser power (W) and powder flow rate (g/min).

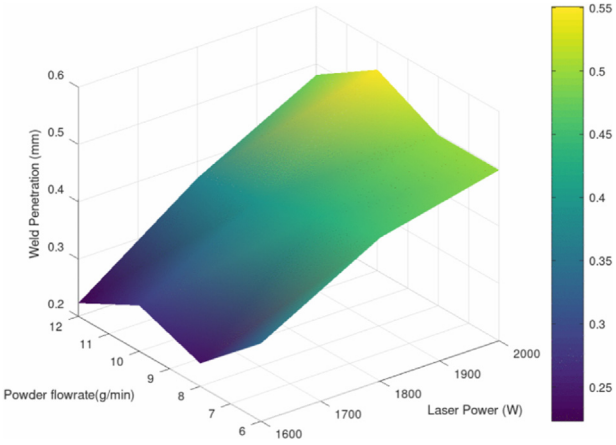


Fig. 11. Ti-6Al-4V single track penetration (mm) against laser power (W) and powder flow rate (g/min).

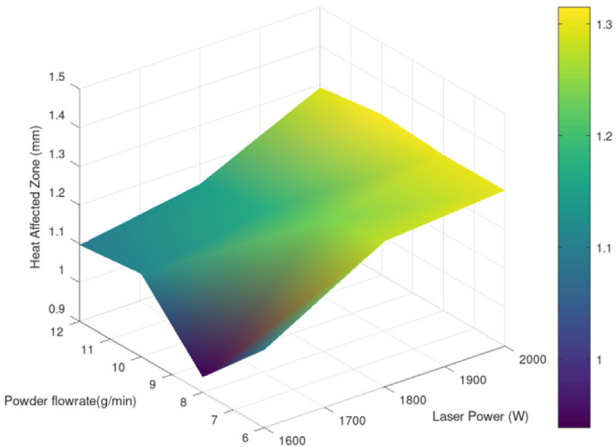


Fig. 12. Ti-6Al-4V single track HAZ (mm) against laser power (W) and powder flow rate (g/min).

grains [12]. The dark areas seen on the multi-layer titanium sample are attributed to over etching of the grain boundaries, rather than being cracks.

It is worth noting that for depositions performed using titanium, while the oxygen reading prior to deposition is assumed

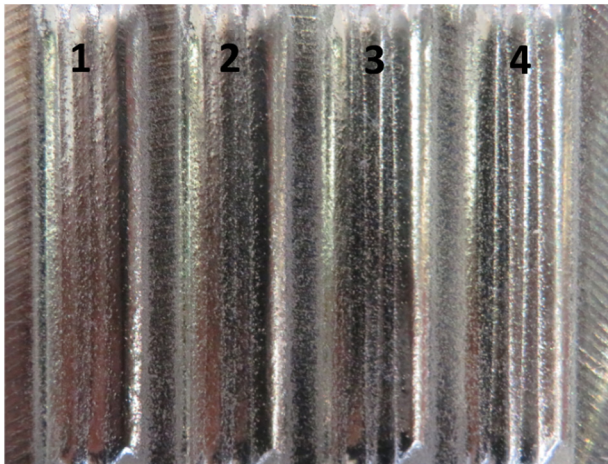


Fig. 13. Ti-6Al-4V multi-track layer sample.

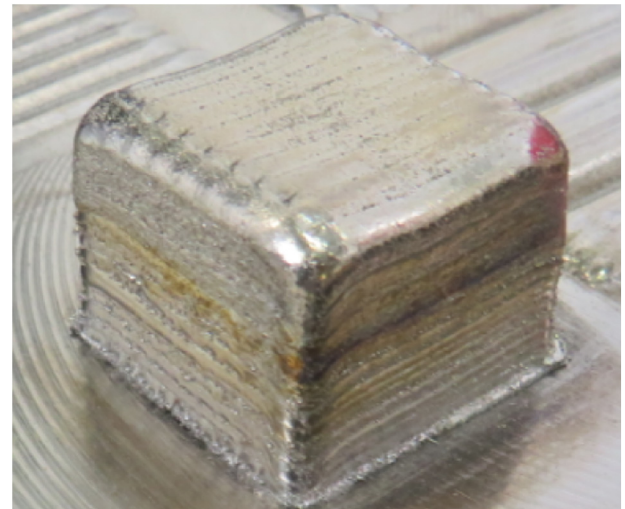


Fig. 15. Image of the multi-layer Ti-6Al-4V sample 30 × 30 × 25 mm in size.

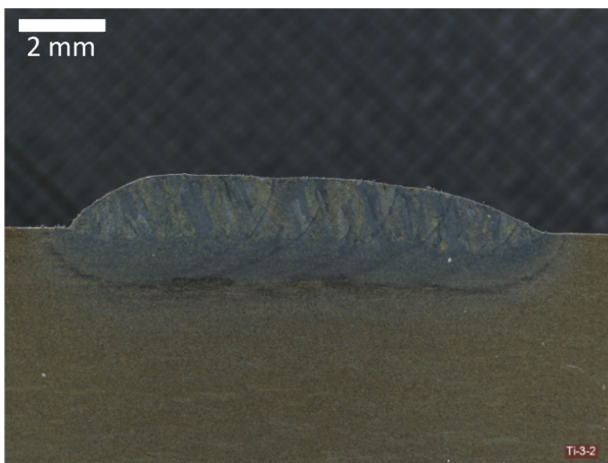


Fig. 14. Sectioned, etched view of a Ti-6Al-4V multi-track layer sample.

to be accurate. During deposition of titanium, hydrogen is emitted which has been noted to cause zirconium oxygen sensors to read near zero. This may not have been the case for these experiments as only a relatively small amount of titanium was deposited and sensor was located slightly away from the deposition to avoid damage from the heat of the process. This aside, material content analysis showed a deposited multi-layer titanium sample had an

oxygen content of 0.079% and nitrogen content of 0.009%. This suggests that the shielding provided by the bag during deposition was low enough to avoid detrimental levels of oxygen and nitrogen absorption, but also that the oxygen content of the stock powder must also have been low. Jun Yu et al. [6] tested a deposited Ti-6Al-4V part for oxygen level using instrumental gas analysis (IGA). The result here was 0.13 wt%, a 0.038 wt% increase comparing with of the powder used.

The bag set-up successfully enabled deposition of titanium on the DMG Mori Lasertec 65 3D Hybrid . It was shown that using this method depositions of over 30 min was possible, without damage being caused to the bag. However, the setup of this solution is time consuming and the effectiveness of it, in terms of the achievable minimum oxygen level and durability, is down to the user when constructing.

One step on theDMG Mori Lasertec 65 3D Hybrid that could improve the effectiveness would be to use a smaller nozzle. This is an option currently commercially available on the Lasertec 65 3D, where the standard 3.2 mm wide nozzle can be exchanged for a 1.6 mm wide nozzle. This nozzle has been designed for the deposition of small features and thin wall structures, however, as seen in the work completed by J. Yu et al. [6] the use of lower powder flow rates can be beneficial for limiting oxidation. This effectively results in an increased shielding gas flow rate to powder flow ratio but also the lower laser power required for the small nozzle will reduce the oxygen absorption as not as much heat will be retained in the part during the process. The downside to using the smaller nozzle being a reduction in the material deposition rate.

Table 5
Parameters and probing data for Ti-6Al-4V multi-track layer samples.

No.	Laser power (W)	powder flow rate (g/min)	x/y step over (mm)	Measured layer height (mm)			
				1	2	3	Average
1	1800	8	1.5	0.958	0.966	1.124	1.016
2	1800	10	1.5	1.117	1.145	1.311	1.191
3	2000	10	1.5	1.148	1.157	1.572	1.292
4	2000	12	1.5	1.146	1.161	1.559	1.289

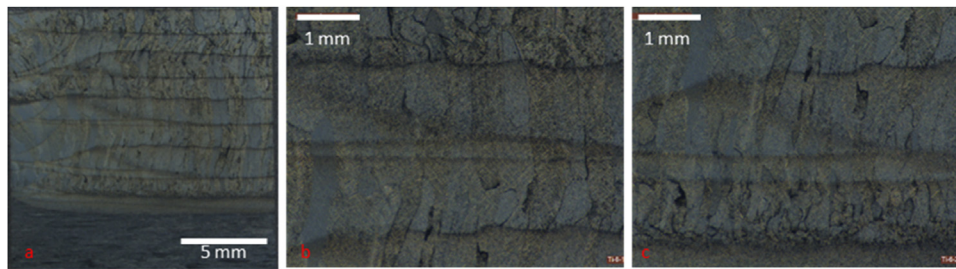


Fig. 16. Ti-6Al-4V multi-layer: a) macro view, b) micro view, c) micro view of first layers.

Conclusion

From the findings presented in this paper the following conclusions have been drawn:

- Deposition of stainless steel 15-5 PH and Inconel 718 was completed using bath, diffused bath and bag shielding set-ups and compared with standard deposition through visual inspection, oxygen sensor data and micrographs. Results from these trials showed that the best performing solution to limit oxidation of the samples was the bag solution.
- Using the bag solution oxygen levels of 100 PPM were possible, compared to 10,000 PPM when using the bath design. For longer depositions, the durability of the bag was tested, in some cases resulting in a rise in oxygen level present in the bag.
- Titanium samples were deposited using the bag design. Low levels of oxidation were visible on the sample surfaces. From the deposition of lines and layers, parameters were down selected and a multi-layer sample of $30 \times 30 \times 25$ mm was deposited.
- Analysis of the titanium samples was completed through sectioning of the lines, layers and multi-layer samples to check for defects and observe the microstructure and also through content analysis.
- The sectioned titanium samples showed no signs of porosity or cracking, with large columnar grains seen in the microstructure that grew epitaxially along the deposition direction and span multiple layers.
- The oxygen content of the multi-layer titanium sample was found to be 0.079%. This means that the material complies with the required oxygen content for grade 5 (0.2%) and grade 23 (0.13%).
- It was noted that whilst the bag setup used in these trials was successful in limiting oxygen absorption to acceptable levels a more robust and repeatable system is required.
- It was also noted that the use of the smaller deposition nozzle could be beneficial in reducing oxygen absorption due to relatively higher shielding and lower heat input when compared with the larger nozzle.

Declaration of interests

The authors declare that they have no known competing financial interests or personal relationships that could have appeared to influence the work reported in this paper.

References

- [1] Yusuf, S.M., Gao, N., 2017, Influence of energy density on metallurgy and properties in metal additive manufacturing. *Mater Sci Technol*, 33/11: 1269–1289.
- [2] Saboori, A., Gallo, D., Biamino, S., Fino, P., Lombardi, M., 2017, An overview of additive manufacturing of titanium components by directed energy deposition: microstructure and mechanical properties. *Appl Sci*, 7/883: 1–23.
- [3] BeAM, "Magic 800," 2020. [Online]. Available: <https://www.beam-machines.com/products/magic800>.
- [4] Optomec, "LENS CS 800 System," 2020. [Online]. Available: <https://optomec.com/lens-cs-800-system/>.
- [5] Zhang, L.-C., Attar, H., 2016, Selective laser melting of titanium alloys and titanium matrix composites for biomedical applications: a review. *Adv Eng Mater*, 18/4.
- [6] Yu, J., Rombouts, M., Maes, G., Motmas, F., 2012, Material properties of Ti6Al4V parts produced by laser metal deposition. *Phys Procedia*, 39:416–424.
- [7] Saboori, A., Biamino, S., Lombardi, M., Tusacciu, S., Busatto, M., Lai, M., Fino, P., 2019, How the nozzle position affects the geometry of the melt pool in directed energy deposition process. *Powder Metall*, 62/4: 213–217.
- [8] Liu, S., Shin, Y.C., 2018, Additive manufacturing of Ti6Al4V alloy: a review. *Mater Des*, 164.
- [9] Kim, H., Lee, B.-S., Seok-Hong, M., Jung, K.-H., Chang-Woo, L., 2017, Atmosphere gas carburizing for improved wear resistance of pure titanium fabricated by additive manufacturing. *Mater Trans*, 58/4: 592–595.
- [10] Hild, E., 2016, Shielding the weld. *MoldMaking Technol*, (June). p. toolweld-micro.com.
- [11] Lindwall, G., Wang, P., Kattner, U.R., Campbell, C.E., 2018, The effect of oxygen on phase equilibria in the Ti-V system: impacts on the AM processing of Ti alloys. *Addit Manuf Ti Comp*, 70:1692–1705.
- [12] Azarniya, A., Colera, X.G., Mirzaali, M.J., 2019, Additive manufacturing of Ti6Al4V parts through laser metal deposition (LMD): process, microstructure, and mechanical properties. *J Alloys Comp*, 804:163–191.
- [13] Hua, T., Jing, C., Fengying, Z., Xin, L., Weidong, H., 2009, Microstructure and mechanical properties of laser solid formed Ti-6Al-4V from blended elemental powders. *Rare Metal Mater Eng*, 38/4: 574–578.
- [14] Keist, J.S., Palmer, T.A., 2016, Role of geometry on properties of additively manufactured Ti-6Al-4V structures fabricated using laser based directed energy deposition. *Mater Des*, 106:482–494.
- [15] Leino, M., Pekkarinen, J., Soukka, R., 2016, The role of laser additive manufacturing methods of metals in repair, refurbishment and remanufacturing – enabling circular. *Phys Procedia*, 83:752–760.
- [16] Sun, J., Zhao, Y., Yang, L., Zhao, X., Qu, W., Yu, T., 2019, Effect of shielding gas flow rate on cladding quality of direct laser fabrication AISI 316L stainless steel. *J Manuf Process*, 48:51–65.
- [17] American Welding Society, "Specification for Fusion Welding for Aerospace Applications," Vols. AWS D17.1/D17.1M:2010-AMD1, 2010.
- [18] Amado, J., Rodríguez, A., Montero, J., Tobar, M., Yáñez, A., 2019, A comparison of laser deposition of commercially pure titanium using gasatomized or Ti sponge powders. *Surf Coat Technol*, 374:253–263.
- [19] Eo, D.-R., Park, S.-H., Cho, J.-W., 2020, Controlling inclusion evolution behavior by adjusting flow rate of shielding gas during direct energy deposition of AISI 316 L. *Addit Manuf*, 33.
- [20] Bergmann, J.P., 2004, Influence of the oxygen content in the shielding gas on microstructure and mechanical properties of laser welds of titanium and titanium alloys. *Werkstofftech*, 35/9.
- [21] Abioye, T.E., Farayibi, P.K., Clare, A.T., 2017, A comparative study of Inconel 625 laser cladding by wire and powder feedstock. *Mater Manuf Process*.
- [22] Occupational Safety and Health Standards, "Personal Protective Equipment; Respiratory Protection - Standard number:1910.134," [Online]. Available: <https://www.osha.gov/laws-regs/regulations/standardnumber/1910/1910.134>. [Accessed 06 2020].
- [23] Guo, P., Zou, B., Huang, C., Gao, H., 2017, Study on microstructure, mechanical properties and machinability of efficiently additive manufactured AISI 316L stainless steel by high-power direct laser deposition. *J Mater Process Tech*, 240:12–22.